Geochemical Evaluation of Thermal Maturity and Depositional Palaeoenvironment of Seven Cretaceous Formations from the East Sirt Basin, Libya

S. Aboglila*, K. Grice, K. Trinajstic, D. Dawson, K. Williford

Abstract: The Sirt Basin is Libya's most important petroleum province and the world's 13th largest petroleum-producing region. Several potential source rocks have been recognised within a complex geological setting, ranging in age from Precambrian to Eocene. Biomarker ratios, together with stable carbon ($\delta^{13}C$) and hydrogen (δD) isotopic compositions of individual hydrocarbons in source rock extracts (n = 21) from the East Sirte Basin were used to establish their thermal maturity and palaeoenvironmental conditions of deposition. Rock Eval pyrolysis data (OI range: 3 - 309 mg CO_2/g TOC and HI range: 115 – 702 mg/hydrocarbon/ g TOC) obtained from source rocks of the Cretaceous Sirte, Tagrifet, Rakb, Rachmat, Bahi and Nubian formations show that the organic matter (OM) is mainly dominated by Type II/III kerogen. Vitrinite reflectance data (% R_o range: 0.46 – 1.38) support variations in thermal maturity and indicate mature to post mature rocks in the Sirte and Rachmat Formations and early to mid stage maturities for the other formations. The Sirte Formation in the study area was found to be relatively more thermally mature than the Tagrifet, Rakb, Rachmat, Bahi, and Nubian Formations, reflected by δD of pristane (Pr) and phytane (Ph) (less depleted in D). A contribution of terrigenous organic matter to all formations except the Sirte Formation is evident from δD of the higher-molecular-weight *n*-alkanes. Anoxic and suboxic of the source rock deposition was identified via the pristane to phytane (Ph/Ph range 0.65 – 1.25) and dibenzothiophene to phenanthrene (DBT/P range 0.04 – 0.47) values.

Keywords*:* Sirt Basin, Source rocks, Biomarker, Pyrolysis, Kerogen, Stable isotopes.

INTRODUCTION

The Sirt Basin is one of Africa's most productive oil provinces, located in north-central Libya. It occupies an area of 600,000 km^2 (Abadi, 2002), and is the 13th largest petroleum region (Ahlbrandt, 2001), with oil equivalent recoverable in reserves of approximately 43 billion barrels (Burwood *et al* 2003) (Fig. 1). Reviews of reserves, stratigraphy structure, and petroleum geological descriptions have been reported by many authors (e.g., Ghori and Mohammed, 1996; Baric *et al* 1996; Ahlbrandt, 2001; Burwood *et al* 2003, Aboglila *et al* 2010)

Several petroleum systems have been identified, migrated-marginal to the horsts and the deeper Agedabia grabens in the offshore areas of the basin (Baird *et al* 1996, Hallett, 2002). Petroleum in the Eastern Sirt Basin occurs in Mesozoic clastic reservoirs, in stratigraphic traps superimposed on structural highs, such as those of the Sarris and Massla fields (Abadi, 2002) (Fig. 1). The main structural features are the Upper Mesozoic–Cenozoic Agedabia and the slightly older Lower Cretaceous Hameimat, Maragh and Sarir Troughs (Burwood *et al* 2003) (Fig. 1). Subsidence throughout the Mesozoic resulted in basin-fill sediments hosting source rocks (Burwood *et al* 2003). Sediments decrease in thickness from 7 km offshore in the northern Gulf or Sirte province to around 1 km near the Nubian uplift in the south (Ahlbrandt, 2001). The grabens, particularly those in the southern part of the Zallah (Abu Tumayam), Maragh (Marada) and Sirte grabens, have recently been identified as potential hydrocarbon kitchens (Hallett and El-Ghoul, 1996).

Hydrocarbons generated by Upper Eocene carbonate source rocks, particularly offshore, offers additional hydrocarbon potential (Gruenwald, 2001). Traditionally, Upper Cretaceous marine shales of the Sirte and Rachmat Formation were identified as the main source rocks for hydrocarbons in the Sirte Basin (Ghori and Mohammed, 1996;

*Corresponding Authors. Fax: +218217316202. E-mail address: Salem.aboglila@gmail.com

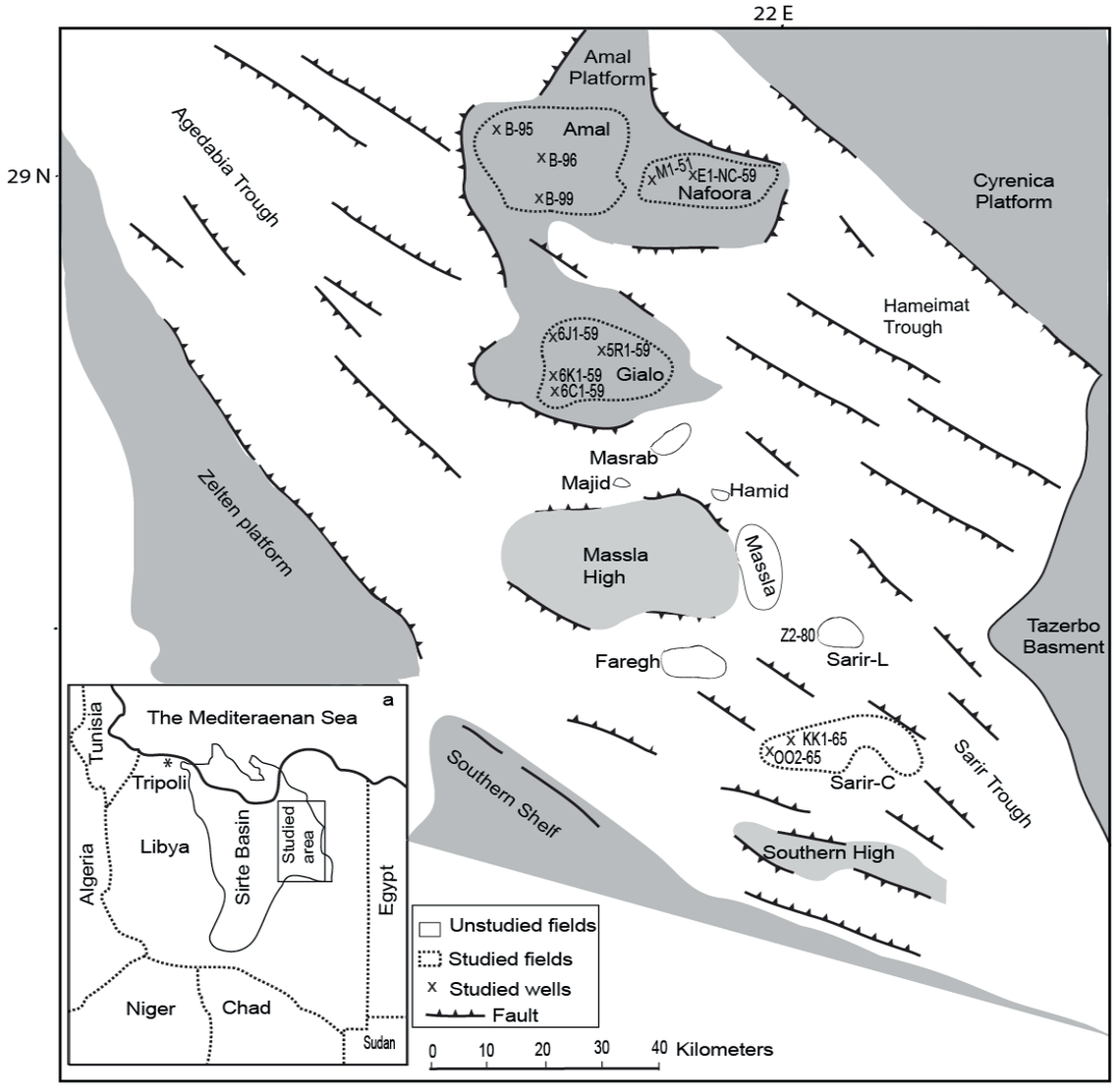

Fig. 1. Map shows the location of the Sirt Basin and its structural elements illustrate regional faults, high troughs and well samples in the studied area. Modified from Ahlbrandt (2001) and Aboglila *et al* (2010).

Baric *et al* 1996) (Fig. 2), with total organic carbon (TOC) contents ranging between 1 and 5% (El-Alami *et al* 1989). The main depocentre in the East Sirt Basin is the Agedabia Trough (Fig. 1) and due to the thickness of the section (>1400 m), source rock maturity differs between the basal and uppermost shales (Burwood *et al* 2003). Vitrinite reflectance (R_o) data indicate that the main source rocks have reached at least three levels of thermal maturity (Hallett, 2002). Basin modelling shows that in the southern part of the Agedabia Trough the Rachmat Formation entered the oil window during the Mid-Eocene, whereas the Sirte Shale started generating oil in the Late Eocene. In the north of the Agedabia Trough (Fig. 1), where it plunges steeply the sediments are post mature and have generated gas (Burwood *et al* 2003). Upper Cretaceous marine shales of the Rakb Formation and the carbonates of the Tagrifet Formation (Fig. 2) have been identified as source rock candidates in the Hameimat Trough; and the Rakb Formation is believed also to act as the seal for a number of the Sarir fields. The Nubian Formation (Triassic and Lower Cretaceous) (Fig. 2) comprises mostly continental sandstones, although some lacustrine shale horizons, located in the Faregh and Massla field of the Hameimat Trough (Fig. 1), may also act as source rocks for minor amounts of waxy oil in the southern part of the Agedabia Trough (El-Hawat *et al* 1996; Burwood *et al* 2003).

The purpose of this paper is to improve characterization of Cretaceous shale source rocks in the East Sirt Basin (Figs 1-2). An organic geochemical assessment of 99 source rock samples

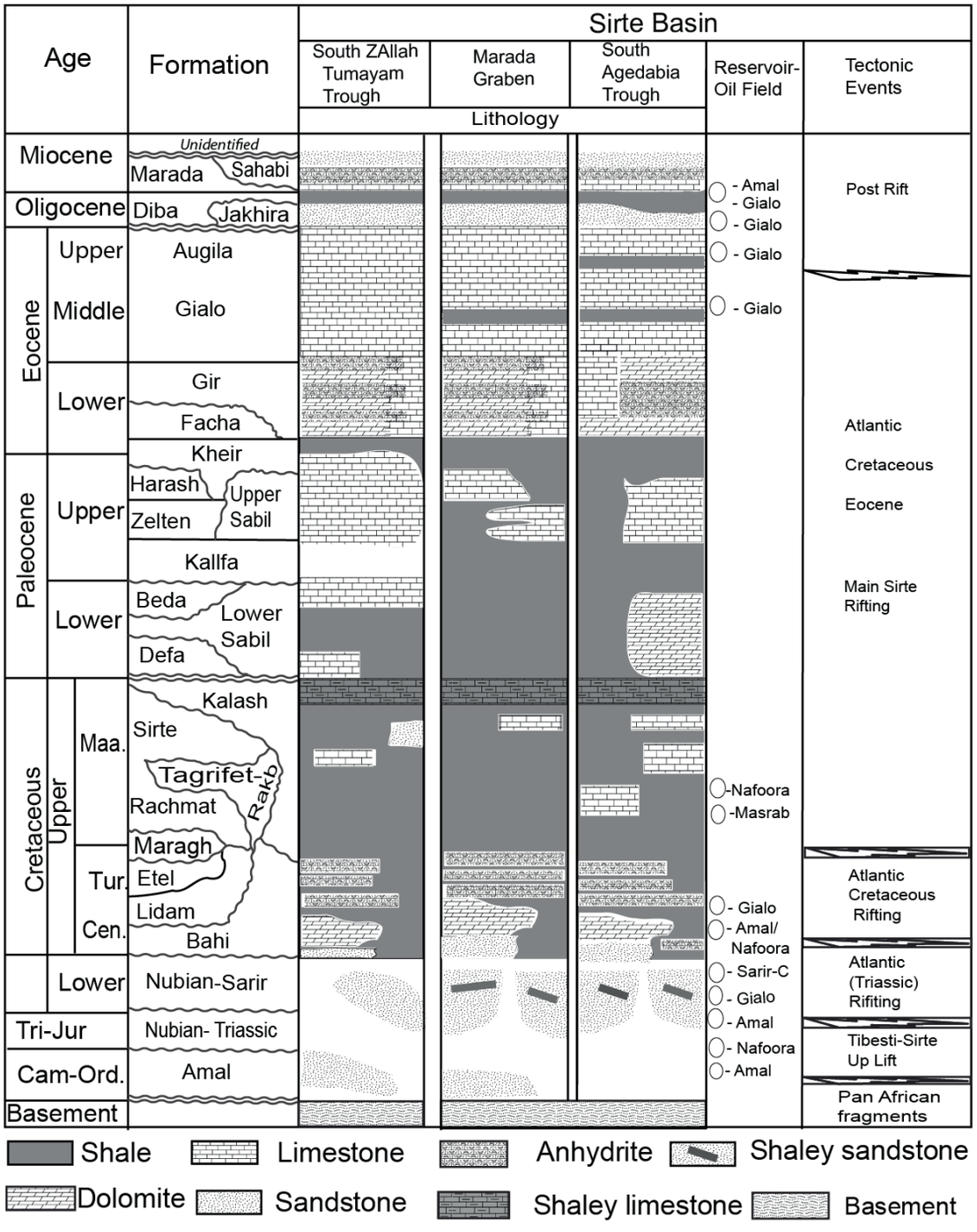

Fig. 2. Stratigraphic column of the Sirt Basin highlighting the lithologies of the formations, the reservoir units of the oil fields demonstrates age, formations, lithology, main reservoir-oil fields and its tectonic events. Modified from Barr and Weeger (1972), Burwood *et al* (2003) and Aboglila *et al* (2010).

(n = 99) was performed on seven Cretaceous formations. Twenty-one of these samples were subjected to more detailed biomarker and compound-specific stable carbon and hydrogen isotopes analyses. From these data, the relative thermal maturities and paleoenvironments of deposition of the source rocks were established.

MATERIALS AND METHODS

Geological setting: The Sirt Basin is part of one of Africa's oldest Hercynian structural provinces (Gras, 1996). Alternating episodes of uplift and subsidence commenced in the Neoproterozoic with the Pan-African orogeny that consolidated a

number of proto-continental fragments into an early Gondwanaland (Kroner, 1993). Rifting began in the Early Cretaceous, peaked in the Late Cretaceous, and ended in the Early Tertiary, resulting in the triple junction within the basin (Ahlbrandt, 2001). During the Late Jurassic and Early Cretaceous, the central Atlantic Ocean opened between northwest Africa and North America, which led to a westward shift of the African plate relative to the European plate. At this time, continental rifting was active in Africa, affecting the Northeast Brazil-Gulf of Guinea domain, southern Chad, Sudan, Kenya, the north and east of Niger, the western desert of Egypt and the southern Sirt Basin in Libya (Coward and Ries, 2003). The east-west trending structures of the Sarir and Hameimat Trough of the Sirt Basin were formed during this period (Guiraud and Maurin, 1991).

Samples: Ninety-nine samples of drill cuttings were collected by the National Oil Corporation (NOC) in Tripoli from 11 different wells (Fig. 1), located in the Amal, Gialo, Nafoora, and Sarir Fields. The attached NOC report confirmed that all samples are uncontaminated with Drilling additives. The units sampled were the Upper Cretaceous Kalash Sirte, Rakb, Tagrifet Rachmat and Bahi Formations (Fig. 2) and the Lower Cretaceous Nubian (Sarir) Formation (Fig. 2). The terms Nubian Sandstone and Sarir Formation have been used by many authors for all or part of the non-marine Lower Cretaceous units (c.f., Hallett, 2002).

Preparation of cutting samples: The cutting samples were washed with doubly distilled water and dried at room temperature prior to analysis. For more confirmation, group of random samples were sent to determine rocks contamination with drilling Fluid by gas chromatography-mass spectrometry. Following Rock-Eval pyrolysis and TOC analysis (see below), a suite of representative samples was selected for more detailed organic geochemical examination. These samples were ground to a fine powder (particle size of <150 μm) using a ring-mill (Rocklabs).

Rock-Eval pyrolysis and total organic carbon (TOC) measurements: Rock-Eval pyrolysis of powdered rock (10-50 mg) was carried out on a Girdel Rock-Eval instrument, while the TOC was measured on a Leco instrument. Samples with low TOC values (< 0.5%) were considered unsuitable for Rock-Eval pyrolysis and therefore not subjected to further analyses.

Solvent extraction and isolation of the maltenes: Twelve cuttings samples from representative formations were selected for solvent extraction based on TOC values (> 0.3%). About 10-20 g of ground sediment was extracted in an ultrasonic bath for two hours using a 9:1 mixture of dichloromethane (DCM) and methanol (MeOH). The solvent extract was then filtered and excess solvent removed by carefully heating on a sand bath (60°C) to obtain the bitumen. Asphaltenes were precipitated by mixing the bitumen with an excess of chilled *n*-heptane. The mixture was left (1 h) to settle for 1 h and later centrifuged at 2500 rpm for 5 min. The supernatant solution containing the maltenes was carefully decanted. This procedure was repeated (5x) by adding fresh *n*-heptane to precipitate the asphaltenes. Maltenes from the bitumens were fractionated using a small-scale column chromatographic method (Bastow *et al* 2007). In brief, the sample (maltenes, about 10–20 mg) was applied to the top of a small column (5.5 cm x 0.5 cm i.d.) of activated silica gel (120°C, 8 h). The aliphatic hydrocarbon (saturated) fraction was eluted with *n*-pentane (2 mL); the aromatic hydrocarbon fraction with a mixture of *n*-pentane and DCM (2 mL, 7:3 v/v,); and the polar (NSO) fraction with a mixture of DCM and MeOH (2 mL, 1: 1 v/v).

5A Molecular sieving: Aliphatic fractions of maltenes were subjected to 5A molecular sieving as described by Grice *et al (*2008). In brief, a portion of the aliphatic fraction in cyclohexane was added to a 2 mL vial, filled with activated sieves (7 mg). The vial was sealed and placed into a pre-heated aluminum block (85°C, 8 h). The solution was then cooled and decanted through a small column of silica plugged with cotton wool and pre-rinsed with cyclohexane (2 mL). The sieves were subsequently rinsed well with cyclohexane and the washings filtered through the same silica column. The combined filtrates yielded the branched/ cyclic fraction. The *n*-alkanes were recovered by hydrofluoric acid (HF) digestion of the sieve as described previously (Dawson *et al* 2005).

Gas chromatography–mass spectrometry (GC-MS): Aliphatic and aromatic fractions were analysed by GC-MS using a Hewlett Packard (HP) 5973 mass-selective detector (MSD) interfaced to a HP6890 gas chromatograph (GC). A HP-5MS (J and W Scientific) GC column (5%

phenylmethylsiloxane stationary phase) was used with helium as the carrier gas. The GC oven was programmed from 40°C to 310°C at 3˚C/min, after which it was held isothermal for 30 min. Samples were dissolved in *n*-hexane and introduced by the HP6890 autosampler into a split-splitless injector operated in the pulsed-splitless mode. Biomarker data were acquired in a full-scan mode (*m/z* 50-500). The ion source was operated in electron ionization (EI) mode at 70 eV. Selected ion monitoring (SIM) was used to identify the terpanes, steranes and triaromatic steroids by monitoring *m/z* 191, 217, 218 and 231 ions. Selected aromatic compounds were identified using *m/z* 178 (phenanthrene), *m/z* 156 (dimethylnaphthalenes) and *m/z* 184 (dibenzothiophene) ions and relative retention time data reported in the literature.

GC–isotope ratio mass spectrometry (GC-ir-MS): A HP6890 gas chromatograph (GC) equipped with a HP6890 autosampler was used in tandem with a Micromass isotope ratio monitoring mass spectrometer (ir-MS) for stable carbon and hydrogen isotope measurements. The GC-ir-MS conditions used were those detailed by Dawson *et al* (2005). In brief, the GC oven was programmed from 50°C to 310°C at 3˚C/min with initial and final hold times of 1 and 20 min, respectively. An identical capillary column to that used in GC-MS analysis was employed for GC-ir-MS. The carrier gas was He at a flow rate of 1mL/min. The ^{13}C data were obtained by integrating the masses 44, 45 and 46 in the ion currents of the CO_2 reference. CO_2 was produced from oxidation of each chromatographically separated component, after being passed through a quartz furnace packed with copper oxide pellets (heated at 850°C). The accuracy and precision of $\delta^{13}C$ measurements were monitored by analysing a mixture of organic reference compounds having known $\delta^{13}C$ ratios. Each sample was analysed at least three times, and the average $^{13}C/^{12}C$ values and standard deviations are reported in ‰ relative to a CO_2 reference gas calibrated to the Vienna Peedee Belemnite (VPDB). The δD values were obtained by integration of the mass 2 and 3 ions derived from H_2 reference, produced from pyrolysis of each chromatographically separated component, after passing through a quartz furnace packed with chromium particles (350-400 µm particle size, heated at 1050°C). The H_3^+ correction was performed by measuring mass 3 at two different H_2 reference gas pressures. Each sample was analysed at least three times, and average δD values and standard deviations are reported in ‰ relative to a H_2 reference gas calibrated to Vienna Standard Mean Ocean Water (VSMOW).

RESULTS AND DISCUSSION

Bulk geochemical parameters: Report of rocks contamination with a drilling additive confirmed the NOC report. Rock-Eval pyrolysis and TOC (%) measurements for the East Sirt Basin rock samples show quite diverse values (Table 1). TOC values from the Sirte Shale Formation range between 0.18% and 5.50%, while TOC values obtained from the Tagrifet Formation range between 0.36% and 5.16%. Three grey-greenish Rakb Shale Formation samples (Amal Field) have TOC values ranging from 1.00% to 1.42% (Table 1). Nineteen samples from the Rachmat Shale have TOC values ranging from 0.60% to 1.90%. One sample from the Bahi

Table 1. range of Rock Eval/TOC data for selected formations from the East Sirt Basin

Formation	Samples	TOC	OI	HI	Tmax	S_2	S_1	PI
Kalash	6	0.21 to 0.28	n.d.	n.d.	n.d.	n.d.	n.d.	n.d.
Sirte	47	0.18 to 5.50	3 - 185	115 - 481	427 - 437	0.27 –21.40	0.16 – 49.60	0.07 – 1.55
Tagrifet	15	0.36 to 5.16	94 - 210	242 - 612	426 - 440	2.01 – 22.80	0.26 – 51.80	0.11 – 0.79
Rakb	3	1.00 to 1.42	91 - 129	208 -415	428 - 434	2.08 – 5.90	0.30 – 1.11	0.09 -0.20
Rachmat	19	0.60 to 1.90	49 - 221	126 - 702	428 - 434	1.18 – 11.46	0.20 – 31.04	0.09 – 0.43
Bahi	1	0.9	309	413	428	2.75	3.92	0.59
Nubian	8	0.23 to 0.69	262 - 280	419 - 433	425 - 426	2.22 – 2.91	3.05 – 3.79	0.54 – 0.58

TOC (wt %): total organic carbon; HI= Hydrogen Index (S_2*100/TOC) and OI= Oxygen Index (S_3*100/TOC); Tmax (°C): maximum pyrolysis temperature yield; S_2: maximum temperature yield (mg HC/g rock); S_1: low temperature hydrocarbon yield (mg HC/g rock); PI: Production Index (S_1/S_1+S_2); n.d. not determined

Formation from M1-51 well (Nafoora Field) has a TOC of 0.90%. Eight samples from the Lower Cretaceous Nubian Formation have TOC values ranging from 0.23% to 0.69%, with the majority having < 0.5% TOC. TOC values < 0.4% indicate low source rock potential. Rock-Eval pyrolysis data for all formations, including S_1 and S_2 (mg HC/g rock), Tmax (°C), production indices (PI), hydrogen indices (HI = mg HC/g TOC) and oxygen indices (OI = mg CO_2/g TOC) were measured. The HI versus OI (Fig. 3) and TOC versus S_2 (Fig. 4) plots are used to determine source rock quality (kerogen type) and richness. The majority of the source rocks contain Type II kerogen (Peters and Moldowan, 1993), while the higher OI values of the Bahi and Nubian Formations indicate mixed Type II-III kerogen. The hydrocarbon potential of East Sirt Basin samples ranges from fair to excellent based on S_2 and TOC (Fig. 4). The Sirte and Tagrifet Formations exhibit the best (good to excellent) hydrocarbon potential. The high values (>1.0) for the S_1 peak (free hydrocarbons) and the abnormally high PI values (>0.2) are indicative of migrated bitumen in (Baird *et al* 1996, Hallett, 2002) or contamination by drilling additives, as observed in other studies (e.g. Shaaban *et al* 2006).

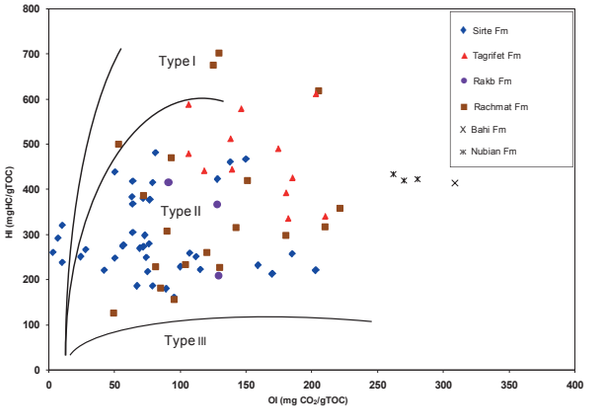

Fig. 3. Plot of hydrogen index (HI) versus oxygen index (OI) illustrating the variation of kerogen type (I, II and III) in source *rocks of the East Sirt Basin.*

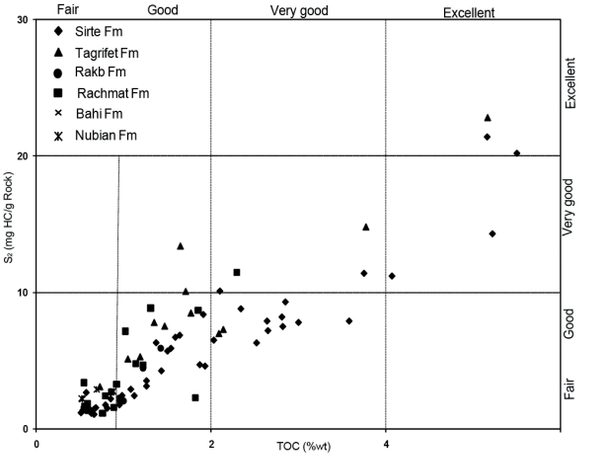

Fig. 4. Plot of Rock-Eval S2 (mg HC/g rock) versus total organic carbon (TOC, wt. %) illustrating the variation of organic richness and petroleum generation potential in source rocks of the East Sirt Basin.

Vitrinite reflectance (% R_o): Vitrinite reflectance is the most extensively used thermal maturity indicator in petroleum geochemistry (e.g. Tissot and Welte, 1984), and was used to evaluate the studied samples. These measurements show some correlation with the depths of the samples. Vitrinite reflectance data of representative samples from the deeper Sirte Formation range from 0.90 and 1.38 %R. Two samples from the deeper Rachmat Formation have %R_o of 0.81 and 0.85. Both the Sirte and Rachmat Formation samples reached the oil window (Table 2), while samples from the shallower Tagrifet, Rakb, Bahi and Nubian Formations have %R_o values ranging between 0.46 and 0.58, supporting an early to mid-stage thermal maturity (Fig. 5).

HYDROGEN AND CARBON ISOTOPIC COMPOSITION

δD of n-alkanes and isoprenoids: Fig. 6 compares the δD signatures of Pr and Ph measured in the various source rock intervals from the East Sirt Basin. Pr and Ph have been shown to become more enriched in D with increasing thermal

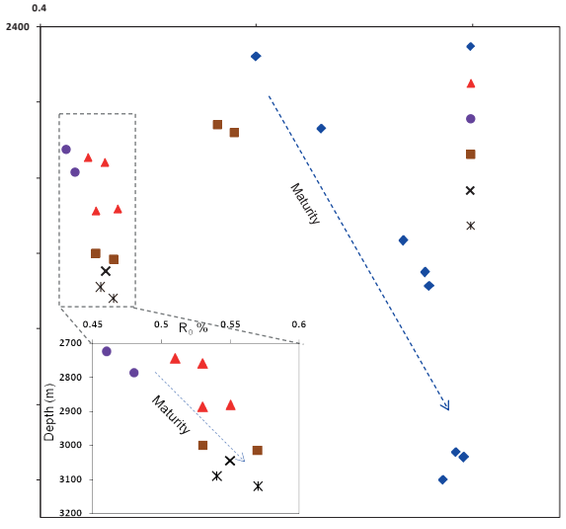

Fig. 5. Plot of vitrinite reflectance versus depth for selected source rock extracts from the East Sirt Basin.

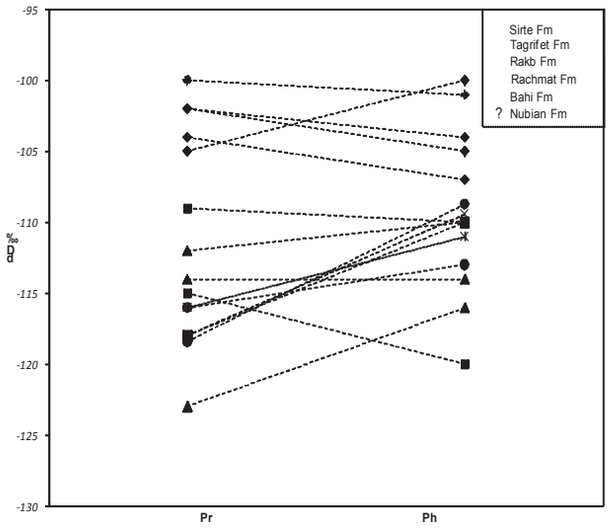

Fig. 6. Stable hydrogen isotopic compositions (δD ‰) of isoprenoid alkanes (Pr and Ph) in selected source rock extracts from the East Sirt Basin.

maturity (Dawson *et al* 2005, 2007; Pedentchouk *et al* 2006). The collected data (Table 2) indicate that δD values of isoprenoids are more positive than n-alkanes. The D enrichment in δD of Pr and Ph can attributed to H/D exchange reactions, which favour the main and minor carbons adjacent to tertiary centres (Pedentchouk *et al* 2006; Dawson *et al* 2007). Isoprenoids tend to undergo hydrogen exchange at tertiary carbons more readily than secondary or primary carbon in straight-chain *n*-alkanes. The mechanism of hydrogen exchange led to D enrichment in pr and ph has known as rearrangement of chiral centres via structural changes in pr and ph isoprenoids (Dawson *et al* 2007).

The observed enrichment of D in the Pr and Ph in these Libyan source rocks shows a strong correlation with various conventional thermal

Table 2. Vitrinite reflectance and stable hydrogen and carbon isotopic data for the source-rocks of the East Sirt Basin.

Field	Well	Formation	Depth (m)	$\%R_o$	Pr (δD‰)	Ph(δD‰)	δD‰	$\delta^{13}C$‰	ΔD‰
Galio	6C1-59	Sirte	3051-54	1.29	-100	-101	-115	-29.2	15
Galio	6C1-59	Sirte	3600-03	1.33	-105	-100	-110	-30	8
Galio	6C1-59	Sirte	3087-90	1.30	-102	-105	n.d.	n.d.	n.d.
Galio	6J1-59	Sirte	3528-31	1.36	-102	-104	-109	-30.1	6
Galio	6J1-59	Sirte	3542	1.38	n.d.	n.d.	n.d.	n.d.	n.d.
Galio	6R1-59	Sirte	2967	1.24	-104	-107	n.d.	n.d.	n.d.
Sarir-C	KK1-65	Sirte	2670	1.05	n.d.	n.d.	n.d.	n.d.	n.d.
Sarir-C	OO2-65	Sirte	2478-81	0.90	n.d.	n.d.	n.d.	n.d.	n.d.
Nafoora	M1-51	Tagrifet	2882	0.58	-123	-116	-92	-31.8	-28
Sarir-C	KK1-65	Tagrifet	2745	0.51	-114	-114	-98	-33.1	-16
Sarir-C	KK1-65	Tagrifet	2760	0.55	n.d.	n.d.	-98	-32.8	n.d
Sarir-C	OO2-65	Tagrifet	2612	0.53	-112	-110	n.d.	-32.1	n.d
Amal	B-96	Rakb	2786	0.48	-118	-109	-92	n.d.	-20
Amal	B-95	Rakb	2725	0.46	-116	-113	n.d.	n.d.	n.d.
Nafoora	M1-51	Rachmat	3015	0.57	-118	-109	-96	-30.9	-18
Nafoora	M1-51	Rachmat	3000	0.53	-109	-110	n.d.	n.d.	n.d.
Sarir-C	OO2-65	Rachmat	2681	0.85	-115	-120	-98	-31.2	22
Sarir-C	OO2-65	Rachmat	2660	0.81	n.d.	n.d.	n.d.	n.d.	n.d.
Nafoora	M1-51	Bahi	3045	0.55	-118	-109	-96	-30.7	-18
Nafoora	M1-51	Nubian	3120	0.57	n.d.	n.d.	n.d.	n.d.	n.d.
Nafoora	M1-52	Nubian	3090-93	0.54	-116	-111	-99	-31	-15

R_o= vitrinite reflectance ; δD‰ = the average of δD values of *n*-alkanes (C_{17} to C_{27}); ^{13}C‰ =the average of $\delta^{13}C$‰ values of *n*-alkanes (*n*-C_{16} to *n*-C_{27}) and ΔD‰ = Difference between average D values of Pr and Ph and average δD values of *n*-alkanes (*n*-C_{17} to *n*-C_{27}); n.d. not determined.

maturity parameters, such as % R_o. Pr and Ph in the Sirte Formation are relatively more enriched in D than isoprenoids in all other formations, having δD values ranging from -100 to -105‰ for Pr and from -100 to -104‰ for Ph. δD for the isoprenoids in the other formations range from -114 to -123‰ for Pr and -120 to -109‰ for Ph (Table 2). These δD data are consistent with the Sirte Formation being the most mature source rock of the East Sirt Basin.

The less mature rocks of the East Sirt Basin (Tagrifet, Bahi, Rakb and Rachmat Formations) contain Ph slightly more enriched in D relative to Pr (Fig. 6); possibly reflecting different sources (i.e. terrigenous plants versus algae) for Pr (cf. Dawson *et al* 2007). The *n*-alkane D profiles of these source rocks are shown in Fig. 7. The δD values of the higher-molecular-weight *n*-alkanes (C_{21}–C_{27}) from the Tagrifet, Bahi, Nubian, Rakb and Rachmat Formations are more positive (-94 to -91‰) than the lower-molecular-weight homologues in the same samples, reflecting perhaps an input to the higher *n*-alkanes from land plants. The samples from the Bahi, Nubian, Rakb, Rachmat and Tagrifet

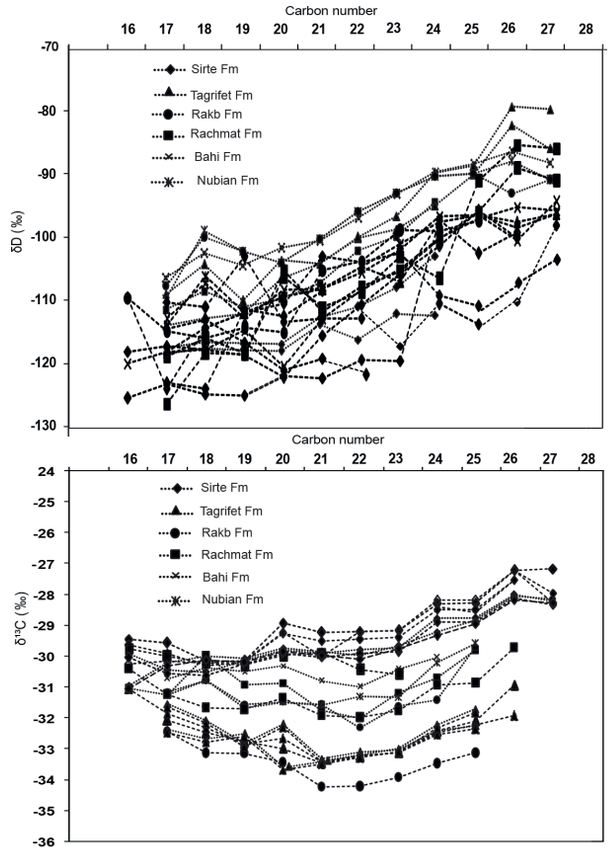

Fig. 7. Stable hydrogen isotopic (δD ‰) and stable carbon isotopic (δ13C ‰) profiles of n-alkanes in selected source-rock extracts from the East Sirt Basin.

Formations contain *n*-alkanes with average δD values from -99 to -92‰, indicating greater input of D-enriched terrigenous OM relative to the more distal (deeper) marine Sirte Formation, which has average δD for *n*-alkanes of -115‰ to -109‰. Sedimentary OM in marine source rocks typically has δD values close to -150‰ if no significant isotopic exchange has occurred during thermal maturation (Santos Neto and Hayes, 1999).

$\delta^{13}C$ of n-alkanes: The $\delta^{13}C$ values of the *n*-alkanes in the source rocks range from -29.2 to -33.1‰ (Table 2) and the *n*-alkane $\delta^{13}C$ profiles are shown in Fig. 7. Stable carbon isotope signatures of n-alkanes can be affected by many factors, such as source of OM (Hayes, 1993; Peters and Cassa, 1994) and thermal maturation (Rigby *et al* 1981; Clayton, 1991). In the Sirte Formation the average $\delta^{13}C$ values of the *n*-alkanes (C_{17}–C_{27}) are significantly heavier (-30.1 to -29.2‰) than those of the same *n*-alkanes in the other formations (-33.1 to -30.7‰). These isotopic differences could be due to differences in thermal maturation and/or source. The preferential generation and expulsion of ^{13}C-depleted hydrocarbons during source rock maturation leads to progressive enrichment of the residual kerogen in ^{13}C (Clayton, 1991). In the case of the Sirte Formation, the heavier $\delta^{13}C$ values of residual *n*-alkanes are most likely due to higher thermal maturity (Fig. 7).

MOLECULAR COMPOSITION

Thermal maturity parameters: Two well-established biomarker parameters (Peters and Moldowan, 1993, Peters *et al* 2005) were used to assess the thermal maturity of selected samples (Table 3). Ts/Ts+Tm values range from 0.41 to 0.62 and 20S/20*S*+20*R* values from 0.22 to 0.58, spanning the onset of oil generation (immature to mature). The highest maturities are displayed by the Sirte Formation in the Gialo field, in agreement with the findings of El-Alami (1996). The Sirte Formation likewise appears to be considerably more mature than other formations studied herein based on measurements of methylphenanthrene index (MPI-1) and calculated vitrinite reflectance (Rc = 0.60 MPI + 0.4: Radke and Welte, 1983). The elevated maturity of the Sirte Formation (R_c = 0.9–1%) in agreement vitrinite reflectance data (above) and from the adjacent Agedabia Trough (R_o ≈ 1.2–2%: Hallet, 2002). Although stratigraphically older, the Tagrifet, Rachmat, Rakb, Bahi and Nubian

Table 3. Geochemical parameters of thermal maturity calculated from the distribution and abundance of aliphatic biomarkers.

Field	Well	Formation	Depth (m)	Ts/Ts +T m	αααC_{29} S/S+R	C_{29} ββ/αββ + αα
Galio	6C1-59	Sirte	3051-54	0.61	0.49	0.83
Galio	6C1-59	Sirte	3600-03	0.62	0.58	1.00
Galio	6C1-59	Sirte	3087-90	0.61	0.50	n.d.
Galio	6J1-59	Sirte	3528-31	0.62	0.50	1.05
Galio	6J1-59	Sirte	3542	0.62	0.50	n.d.
Galio	5R1-59	Sirte	2967	0.58	0.46	n.d.
Sarir-C	KK1-65	Sirte	2670	0.61	0.40	0.91
Sarir-C	OO2-65	Sirte	2478-81	0.50	0.36	n.d.
Nafoora	M1-51	Tagrifet	2882	0.45	0.24	0.24
Sarir-C	KK1-65	Tagrifet	2745	0.54	0.35	0.35
Sarir-C	KK1-65	Tagrifet	2760	0.53	0.36	0.36
Sarir-C	OO2-65	Tagrifet	2612	0.46	0.22	0.22
Amal	B-96	Rakb	2786	0.41	0.24	0.24
Amal	B-95	Rakb	2725	0.39	0.17	n.d.
Nafoora	M1-51	Rachmat	3015	0.47	0.24	0.55
Nafoora	M1-51	Rachmat	3000	0.50	0.35	n.d.
Sarir-C	OO2-65	Rachmat	2681	0.58	0.36	0.58
Sarir-C	OO2-65	Rachmat	2660	0.53	0.42	n.d.
Nafoora	M1-51	Bahi	3045	0.47	0.35	0.63
Nafoora	M1-51	Nubian	3120	0.47	0.33	n.d.
Nafoora	M1-52	Nubian	3090-93	0.48	0.34	0.35

Ts/Ts+Tm= 18α (H)-22,29,30-trisnorhopane/18α(H)-22,29,30-trisnorhopane+17α(H)-22,29,30-trisnorhopane; *S*/*S*+*R*=C_{29}ααα20*S*/ C_{29}ααα20*S* + C_{29}ααα20*R*; C_{29} αββ/αββ+ααα= 5α,14β,17β-24-ethylcholstane 20*R*/ 5α,14α,17α24-ethylcholstane 20*R*.

formations within the Hameimat and Sarir Troughs (Fig. 1) are at the early stages of oil generation (R_c = 0.65–0.76%).

MOLECULAR COMPOSITION INDICATORS OF DEPOSITIONAL ENVIRONMENT.

3Ph/Ph and DBT/P values: The pristane to phytane (Ph/Ph) and dibenzothiophene to phenanthrene (DBT/P) values of the source rocks (Table 4) reveal the nature of their respective depositional settings. Their DBT/P values (0.04–0.47) are characteristic of marine shales, whereas in most samples, the Pr/Ph ratio is <1, indicating deposition under anoxic conditions. The latter are commonly associated with hypersalinity. The slightly higher Pr/Ph values (1.01–1.25) of six shales from the Sirte, Tagrifet, Rakb and Rachmat Formations (Table 4) suggest suboxic depositional conditions.

Triterpanes and steranes: The hopane, tricyclic terpane and sterane distributions of the source rocks (Fig. 8) are far from uniform, reflecting differences in the origin of their OM. For example, the relative abundance of C_{27}, C_{28} and C_{29} regular steranes vary depending on the contributions of marine or lacustrine phytoplankton, green algae and/or land plants to their kerogen (Huang and Meinshein, 1979; Volkman, 2003). The sterane distributions of most of the samples are dominated by the C_{27} homologue, usually attributed to a marine algal source. The sample

Table 4. Geochemical parameters of palaeoenvironments from the distribution and abundance of aliphatic and aromatic isoprenoids for studied formations.

Field	Well	Formation	Depth (m)	Pr/Ph	DBT/P	$C_{19}TT/C_{23}TT$	$C_{24}TeT/C_{23}TT$
Galio	6C1-59	Sirte	3051-54	0.78	0.46	0.17	0.26
Galio	6C1-59	Sirte	3600-03	0.86	0.47	0.15	0.26
Galio	6C1-59	Sirte	3087-90	1.10	0.22	n.d.	n.d.
Galio	6J1-59	Sirte	3528-31	0.68	0.36	0.08	0.35
Galio	6J1-59	Sirte	3542	0.92	0.29	0.11	0.38
Galio	6R1-59	Sirte	2967	0.92	0.27	n.d.	n.d.
Sarir-C	KK1-65	Sirte	2670	0.86	0.31	n.d.	n.d.
Sarir-C	OO2-65	Sirte	2478-81	0.77	0.13	0.10	0.28
Nafoora	M1-51	Tagrifet	2882	0.86	0.16	0.19	0.26
Sarir-C	KK1-65	Tagrifet	2745	1.13	0.19	0.1	0.31
Sarir-C	KK1-65	Tagrifet	2760	1.25	0.11	0.09	0.31
Sarir-C	OO2-65	Tagrifet	2612	0.85	0.13	0.11	0.35
Amal	B-96	Rakb	2786	1.25	0.25	0.11	0.29
Amal	B-95	Rakb	2725	1.01	0.30	n.d.	n.d.
Nafoora	M1-51	Rachmat	3015	0.70	0.13	0.17	0.29
Nafoora	M1-51	Rachmat	3000	1.12	0.11	n.d	n.d.
Sarir-C	OO2-65	Rachmat	2681	0.80	0.21	0.1	0.29
Sarir-C	OO2-65	Rachmat	2660	0.68	0.30	n.d	n.d.
Nafoora	M1-51	Bahi	3045	0.68	0.04	0.09	0.3
Nafoora	M1-51	Nubian	3120	0.68	0.28	n.d.	n.d.
Nafoora	M1-52	Nubian	3090-93	0.65	0.31	0.1	0.31

Pr= pristane/Ph= phytane; DBT= dibenzothiophene/P= phenanthrene; $C_{19}TT/ C_{23}TT= C_{19}$ tricyclic terpane /C_{19} tricyclic terpane + C_{23} tricyclic terpane; $C_{24}TeT/ C_{23}TT= C_{24}$ tetracyclic terpane /C_{24} tricyclic terpane +C_{23} tricyclic terpan *Keywords:* East Sirte

from the Tagrifet Formation in the Nafoora field is an exception, where the C_{28} sterane is co-dominant with the C_{27} and C_{29} steranes (Fig. 8). However, the Tagrifet Formation contains fossil planktonic foraminifera, bryozoans and inoceramid and rudist molluscs, clearly supporting a marine environment. A high $C_{23}/C_{19}TT$ ratio and low relative abundance of $C_{24}TeT$ are features commonly associated with marine shale and carbonate lithofacies (Aquino Neto *et al* 1983). Thus, the low C_{19} TT/ (C_{19} TT + C_{23}TT) and $C_{24}TeT/(C_{24}TT + C_{23}TT)$ in all rock samples studied (Table 4) are consistent with their interpreted marine affinity.

CONCLUSIONS

1 A variety of organic geochemical analyses were applied to set of rock extracts from the East Sirt Basin (Libya). The thermal maturity and palaeoenvironment of deposition was established using Rock-Eval pyrolysis of source rocks and biomarker ratios and compound-specific stable hydrogen and carbon isotopes of individual hydrocarbons of crude oils and source rock extracts.

2 The thermal maturities of the source rocks from the Sirte Formation were found to be

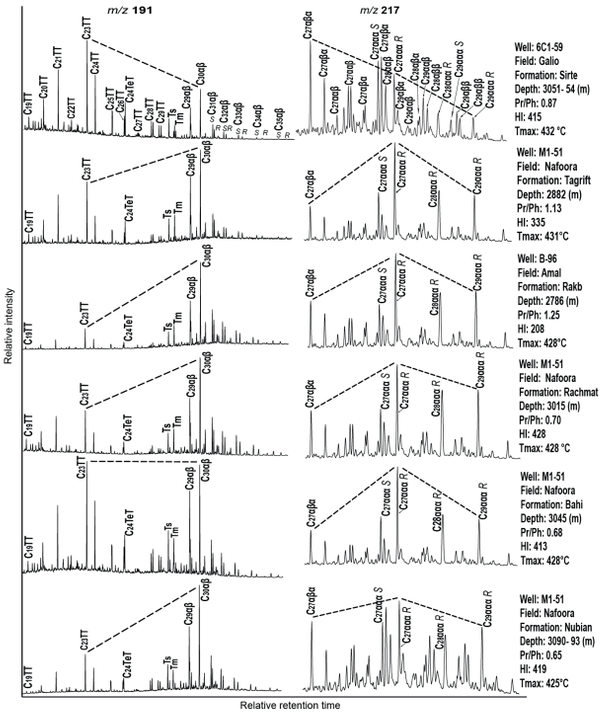

Fig. 8. Partial mass chromatograms showing distributions of tricyclic and tetracyclic terpanes and hopanes (m/z 191) and steranes (m/z 217) in various source rocks in the East Sirt Basin.

higher based on Ts/Ts+Tm (0.61 to 0.62) and $\alpha\alpha\alpha C_{29}$ 20*S*/20*S*+20*R* (0.49 to 0.58) than the Tagrifet, Rakb, Rachmat, Bahi, and Nubian formations. δD differences between *n*-alkanes and isoprenoids (Pr and Ph) are also consistent with higher levels of thermal maturity for the Sirte Formation.

3 Ph/Ph, DBT/P, triterpanes and steranes indicate anoxic to sub oxic depositional environments and variable contributions OM or from marine and lacustrine phytoplankton, green algae and/or land plants to the kerogen in the rocks.

ACKNOWLEDGMENTS

The authors thank Geoff Chidlow and Sue Wang for their assistance with GC-MS and GC-ir-MS analysis, respectively. We are grateful to the staff of the National Oil Corporation (NOC) in Tripoli and staff of the Libyan Petroleum companies (Waha, Veba and Gulf) for providing samples.

REFERENCES

Abadi, A. (2002). Tectonics of the Sirte Basin. *Unpublished PhD Dissertation*, Vrije Universiteit, Amsterdam, ITC, Enschede: p187.

Ahlbrandt, T. S. (2001). The Sirte Basin Province of Libya – Sirte-Zelten Total Petroleum System. *US Geological Survey Bulletin* 2202-F.

Aboglila, S., Grice, K., Trinajstic, K., Dawson, D., Williford, K. (2010). Use of biomarker distributions and compound specific isotopes of carbon and hydrogen to delineate hydrocarbon characteristics in the East Sirte Basin (Libya). *Organic Geochemistry* 41: 1249–1258.

Aquino Neto, F. R., Trendel, J. M., Restle, A., Connan, J., Albrecht, P. (1983). Occurrence and formation of tricyclic and tetracyclic terpanes in sediments and petroleum. In: Bjorøy, M. (Ed.), *Advances in Organic Geochemistry 1981*. John Wiley & Sons Ltd, Chichester, 659-667.

Baird, D. W., Aburawi, R. M., Bailey, N. J. L. (1996). Geohistory and petroleum in the central Sirte Basin. In: M. J. Salem, A. S. El-Hawat and A. M. Sbeta, (Eds.), *Geology of Sirt Basin* II: 3–56.

Baric, G., Spanic, D., Maricic, M. (1996). Geochemical characterization of source rocks in the NC-157 block (Zaltan platform), Sirte Basin. In: M. J. Salem, A. S. El-Hawat and A. M. Sbeta (Eds.), *The Geology of Sirt Basin*, II: 541–553.

Barr, F. T. and Weegar, A. A. (1972). Stratigraphic Nomenclature of the Sirte Basin, Libya. *Petroleum Exploration Society of Libya*, Tripoli, P.179.

Bastow, T. P., Van Aarssen, B .G. K., Lang, D. (2007). Rapid small–scale separation of saturate, aromatic and polar components in petroleum. *Organic Geochemistry* 38: 1235–1250.

Burwood, R., Redfern, J., Cope, M. (2003). Geochemical evaluation of East Sirte Basin, (Libya) petroleum systems and oil provenance. *Geological Society Special Publication*, London, 203–214.

Clayton, C. (1991). Effect of maturity on carbon isotope ratios of oils and condensates. *Organic Geochemistry* 17: 887–899.

Coward, M. P., Ries, A. C. (2003). Tectonic development of North African basins. In: T. Burnham, D. S. MacGregor, N. R. Cameron (Eds.), Petroleum Geology of Africa: New Themes and Developing Technologies, 207. *Geological Society Special Publication*, London: 61-83.

Dawson, D., Grice, K., Alexander, R. (2005). Effect of maturation on the indigenous δD signatures of individual hydrocarbons in sediments and crude oils from the Perth Basin (Western Australia). *Organic Geochemistry* 36: 95–104.

Dawson, D., Grice, K., Alexander, R., Edwards, D. (2007). The effect of source and maturity on the stable isotopic compositions of individual hydrocarbons in sediments and crude oils from the Vulcan Sub-basin, Timor Sea, Northern Australia. *Organic Geochemistry* 38: 1015–1038.

El-Alami, M. (1996). Habitat of oil in Abu Attiffel area, Sirt Basin, Libya. In: M. J. Salem, A. S. El-Hawat and A. M. Sbeta (Eds.), *The Geology of Sirt Basin* II: 337–348.

El-Alami, M., Rahouma, S., Butt, A. (1989). Hydrocarbon habitat in the Sirte Basin Northern Libya. *Petroleum Research Journal* 1: 17–28.

El-Hawat, A. S., Missallati, A. A., Bezan, A. M., Taleb, T. M., (1996). The Nubian Sandstone in Sirte Basin and its correlatives. In: M. J. Salem, A. S. El-Hawat and A. M. Sbeta (Eds.), *The Geology of Sirt Basin* II: 3–30.

Ghori, K. A. R., Mohammed, R. A. (1996). The application of petroleum generation modelling to the eastern Sirt Basin, Libya. In: M. J. Salem, A. S. El-Hawat and A. M. Sbeta (Eds.), *The Geology of Sirt Basin* II: 529–540.

Gras, R., 1996. Structural style of the southern margin of the Messlah High. In: Salem, M.J., El-Hawat, A.S., Sbeta, A.M. (Eds.), *The Geology of Sirte Basin* II. Elsevier, Amsterdam, 201–210.

Grice, K., de Mesmay, R., Glucina, A., Wang, S., (2008). An improved and rapid 5A molecular sieve method for gas chromatography isotope ratio mass spectrometry of n-alkanes (C_8-C_{30+}). *Organic Geochemistry* 39: 284-288.

Gruenwald, R. (2001). The hydrocarbon prospectivity of Lower Oligocene deposits in the Maragh Trough, SE Sirt Basin, Libya. *Jour. Pet. Geo*., 24: 213 231.

Guiraud, R., Maurin, J. C. (1991). Early Cretaceous rifts of Western and Central Africa: an overview. *Tectonophysics* 213: 153–168.

Hallett, D. (2002). Petroleum Geology of Libya. Elsevier, Amsterdam, p. 509.

Hallett, D., El-Ghoul, A. (1996). Oil and gas potential of the deep trough areas in the Sirt Basin, Libya. In: M. J. Salem, A. S. El-Hawat and A. M. Sbeta. (Eds.), *The Geology of Sirt Basin* II: 455–484.

Hayes, J. M. (1993). Factors controlling the ^{13}C contents of sedimentary organic compounds: principles and evidence. *Marine Geology* 113: 111–125

Huang, W. Y. and Meinschein, G. (1979). Sterols and ecological indicators. *Geochimica et Cosmochimica Acta*, 43: 739-745.

Kroner, A. (1993). The Pan-African belt of northeastern and eastern Africa, Madagascar, southern India, Sri Lanka and east Antarctica; Terrane amalgamation during formation of the Gondwana Supercontinent. Geoscientific research in Northeast Africa. *A. A. Balkema, Rotterdam*, Netherlands, 3–9.

Pedentchouk, N., Freeman, K. H., Harris, N. B. (2006). Different response of D values of n-alkanes, isoprenoids, and kerogen during thermal maturation. *Geochimica et Cosmochimica Acta* 70: 2063–2072.

Peters, K. E., Moldowan, J. M. (1993). The Biomarker Guide. Prentice Hall, Eaglewood Cliffs, p. 363.

Peters, K. E., Cassa, M. R. (1994). Applied source rock geochemistry. In: L. B. Magoon, W. G. Dow (Eds.). The Petroleum System-from Source to Trap. *Am. Ass. Petrol. Geol., Memoir* 60: 93–120.

Peters, K. E., Walters, C. C. and Moldowan, J. M. (2005). The Biomarker Guide. Cambridge University Press, Cambridge. P. 1151.

Radke, M. and Welte, D. H. (1983). The methylphenanthrene index (MPI): A maturity parameter based on aromatic hydrocarbons. In: M. Bjorøy (Ed.), *Advances in Organic Geochemistry* 1981. John Wiley & Sons Ltd, Chichester, 504-512.

Rigby, D., Batts, B. D., Smith, J. W. (1981). The effect of maturation on the isotopic composition of fossil fuels. *Organic Geochemistry* 3: 29–36.

Santos Neto, E. V., Hayes, J. M. (1999). Use of hydrogen and carbon stable isotopes characterizing oils from the Potiguar Basin (onshore), Northeastern Brazil. *Am. Ass. Petr. Geol., Bull*., 83: 496–518.

Shaaban, F., Lutz, R., Littke, R., Bueker, C. and Odisho, K. (2006). Source rock evaluation and basin modelling in NE Egypt (NE Nile Delta and Northern Sinai). *Jour. Petrole.* Geo., 29: 103–124.

Tissot, B. P., Welte, D. H. (1984). Petroleum formation and occurrence. Springer-Verlag, Berlin, p 699 .

Volkman, J. K. (2003). Sterols in microorganisms. *Applied Microbiology and Biotechnology*, 60: 495–506.